Journal of Power Sources 217 (2012) 152–157

Contents lists available at SciVerse ScienceDirect

Journal of Power Sources

journal homepage: www.elsevier.com/locate/jpowsour

Graphene-modified polyaniline as the catalyst material for the counter electrode of a dye-sensitized solar cell

Chen-Yu Liu [a], Kuan-Chieh Huang [a], Ping-Hsien Chung [b], Chun-Chieh Wang [a], Chia-Yuan Chen [c], R. Vittal [a], Chun-Guey Wu [c], Wen-Yen Chiu [a,b], Kuo-Chuan Ho [a,b,*]

[a] Department of Chemical Engineering, National Taiwan University, Taipei 10617, Taiwan
[b] Institute of Polymer Science and Engineering, National Taiwan University, Taipei 10617, Taiwan
[c] Department of Chemistry, National Central University, Chung-Li 32001, Taiwan

HIGHLIGHTS

- The effect of refluxed graphene/aniline particles on their dispersibility in a solution is studied.
- Catalytic layers consisting of graphene and polyaniline are prepared for counter electrodes.
- A DSSC with a graphene/polyaniline counter electrode delivers a remarkable efficiency of 7.17%.

ARTICLE INFO

Article history:
Received 7 February 2012
Received in revised form
15 May 2012
Accepted 28 May 2012
Available online 1 June 2012

Keywords:
Counter electrode
Dye-sensitized solar cell
Electro-polymerization
Graphene
Polyaniline

ABSTRACT

A nanocomposite thin film, consisting of graphene (GN) and polyaniline (PANI) (designated as GN/PANI) is coated as a catalytic layer on an FTO glass by electro-polymerization from a solution containing aniline (ANI) monomers and GNs; the thus coated electrode is used as a counter electrode (CE) for a dye-sensitized solar cell (DSSC). Modification of the surface of GNs by the ANI monomers is confirmed by thermo-gravimetric analysis (TGA). Fourier transform spectroscopy (FTIR) and UV/Vis absorption spectra are used to demonstrate the non-covalent interactions between ANI and GN in the GN/ANI particles. The effect of the refluxing process on the dispersibility of GN/ANI particles in an aqueous solution is studied. The high electro-catalytic ability of GN/PANI-CE is established through cyclic voltammetry (CV) and electrochemical impedance spectroscopy (EIS). The short-circuit current density (J_{SC}) and power-conversion efficiency (η) of the DSSC with the GN/PANI-CE are measured to be 16.28 mA cm^{-2} and 7.17%, respectively, while the corresponding values are 15.01 mA cm^{-2} and 7.24% for a DSSC with a CE having Pt as the catalytic material (Pt-CE). The composite film of GN/PANI is thus established to be a potential catalyst for replacing the expensive, conventional Pt in a DSSC.

1. Introduction

The structure of a dye-sensitized solar cell (DSSC) consists of a dye-adsorbed nanocrystalline TiO_2 photoanode, an electrolyte, and a counter electrode (CE) [1]. The CE is a crucial component for achieving high performance for a DSSC. A thin film of Pt is generally used as the catalytic layer on the CE, due to its excellent electro-catalytic ability and high conductivity. The thin film of Pt is usually coated on a transparent conductive oxide glass, e.g., indium-doped tin oxide (ITO) or fluorine-doped tin oxide (FTO) for preparing the CE of a DSSC. As Pt is very expensive, alternative materials, such as carbon materials or conducting polymers, have been extensively investigated in recent years as the catalytic materials for the CEs of DSSCs. Carbon materials, in the forms of carbon nanotubes (CNT) [2], graphite [3], active carbon [4], and graphene (GN) [5–7], have been proposed as alternative catalytic materials for the CEs of DSSCs, because of their good conductivities. Among them, GN, a single-layer material of sp^2-bond-carbon atoms in a hexagonal lattice, has drawn much attention for its engineering applications. GN was noticed to have some unique physicochemical properties, such as high surface area, excellent thermal conductivity, strong mechanical strength, and good electric conductivity [8–10]. On the other hand, conducting polymers, such as poly(3,4-ethylenedioxythiophene)-poly(styrene sulphonate) (PEDOT:PSS) [11,12], poly(3,3-diethyl-3,4-dihydro-2*H*-thieno-[3,4-b] [1,4]dioxepine) (PProDOT-ET$_2$) [13],

* Corresponding author. Department of Chemical Engineering, National Taiwan University, Taipei 10617, Taiwan. Tel.: +886 2 2366 0739; fax: +886 2 2362 3040.
E-mail address: kcho@ntu.edu.tw (K.-C. Ho).

0378-7753/$ – see front matter © 2012 Elsevier B.V. All rights reserved.
http://dx.doi.org/10.1016/j.jpowsour.2012.05.091

polypyrrole [14,15], and polyaniline (PANI) [16,17], have also been incorporated into the CEs for DSSCs. Among them, PANI is considered to be an important electronic conducting polymer due to its desirable characteristics: low cost, environmental stability, high degree of processability, and interesting redox properties [18,19].

Composites of carbon materials and conducting polymers have been used as the catalytic layers on the CEs of DSSCs [20–23]; the superior electro-catalytic activity and conductivity of such catalytic layers render high performance to the DSSCs. In this study, the composite film of GN/PANI was coated on the FTO glass by electropolymerization, using an aqueous solution containing GN and aniline (GN/ANI) particles, which were synthesized via a reflux process. The importance of the reflux process for the preparation of the particles of GN/ANI was discussed. The FTO glass coated with the composite film of GN/PANI was used as the CE in a DSSC. The physical adsorption of ANI monomers onto the surface of GNs via non-covalent bonding was verified by thermo-gravimetric analyzer (TGA). High resolution transmission electron microscopy (HR-TEM) was used to demonstrate the shape of GN/ANI. Selected area electron diffraction (SAED) pattern was used to detect the crystalline nature of the GN/ANI particle. Ultraviolet/visible (UV/Vis) absorption and Fourier-transform infrared (FTIR) spectroscopy were employed to verify the physical adsorption of ANI monomers onto GNs. Raman analyses and scanning electron microscopy (SEM) were applied to confirm successful incorporation of GNs in the GN/PANI composite thin film. The electro-catalytic ability of the CE with GN/PANI was characterized both by cyclic voltammetry (CV) and electrochemical impedance spectroscopy (EIS).

2. Experimental

2.1. Materials

A modified Staudenmaier method was used to obtain graphite oxide (GO) from graphite [24]; the thus obtained GO was then subjected to a thermal exfoliation and reduction to finally obtain the GN [25]. ANI monomers, anhydrous LiI, I_2, acetonitrile (AN), and poly(ethylene glycol) (PEG, M.W. = 20,000 g mol^{-1}) were purchased from Merck. Hydrochloric acid (HCl, 37%), ethanol (EtOH, ≧95%), and nitric acid (HNO_3, 65%) were obtained from Sigma–Aldrich. Titanium(IV) isopropoxide (TTIP, +98%), 4-*tert*-butylpyridine (TBP, 96%), and *tert*-butanol (*t*BuOH, 99.5%) were acquired from Acros. 3-methoxypropionitrile (MPN, 99%) was obtained from Fluka. 1,2-dimethyl-3-propylimidazolium iodide (DMPII) was purchased from Solaronix S. A., Aubonne, Switzerland. Chenodeoxycholic acid (CDCA, ≧95%), Nafion®, and valeronitrile (99.5%) were from Sigmal-Aldrich Chemical Company, Inc. Guanidinium thiocyanate (GuSCN, 99%) was obtained from Acros. Bis-(3,3-dimethyl-butyl)-phosphinic acid (DINHOP) was bought from Dyesol. An MF-Millipore mixed cellulose ester membrane (0.45 μm) was purchased from Millipore.

2.2. Preparation of the counter electrodes with pristine polyaniline, pristine graphene, and with the composite film of graphene and polyaniline

ANI solutions containing different amounts of GN were refluxed at around 210 °C for 3 h to prepare the particles of GN/ANI. Composite films of GN/PANI were then electro-polymerized onto FTO substrates (surface resistance = 7 Ω sq^{-1}, Uni-Onward Corp., Taipei, Taiwan) from aqueous solutions containing 1.0 M GN/ANI and 2.0 M HCl, by applying a constant potential of 0.8 V (*vs.* Ag/AgCl/saturated KCl). The electro-polymerization was stopped when the desired amount of charge was passed. The as-prepared FTO substrates with the composite films of GN/PANI were rinsed with HCl solution, dried under air, and then used as the CEs in DSSCs. The pristine PANI film was obtained in the same way as mentioned above. Pristine GN (0.05 g) and 0.5 mL Nafion® were added to 5 mL EtOH, and this solution was kept under sonication in a VCX 500 ultrasonicator at ambient temperature for 20 min. The pristine GN film was prepared from the resulted GN solution by drop-coating it onto an FTO substrate at ambient temperature.

2.3. Preparation of TiO_2 nanocrystalline film and fabrication of the DSSC

For obtaining TiO_2, 72 mL of TTIP was added to 430 mL of 0.1 M HNO_3. The hydrolyzed TiO_2 solution was then stirred and heated to 88 °C for 8 h via a sol–gel process. After cooling the solution to room temperature, it was further subjected to 240 °C in an autoclave for 12 h. By concentrating the autoclaved solution to 13 wt%, a paste consisting of nanocrystalline TiO_2 was obtained. To prevent the film from cracking during drying and to control the pore size of TiO_2, 30 wt% PEG with respect to the amount of TiO_2 was added to the TiO_2 paste [11]. This TiO_2 paste was then coated onto the FTO by a doctor-blade technique. The FTO glass with the TiO_2 film was dried at room temperature and annealed at 450 °C for 30 min. Another TiO_2 layer of same thickness as before was coated on the obtained TiO_2 film, and the twice coated FTO glass was dried and annealed in the same way. A third layer containing light scattering particles of TiO_2 with an average particle diameter of 300 nm was further coated on it and the thrice coated FTO glass was dried and annealed in the same way. The thrice coated TiO_2 film was then immersed in an AN/*t*BuOH (v/v = 1/1) solution containing 0.3 mM of CYC-B11 [26], 10% DMSO, and 75 μM DIN-HOP for 24 h, and its projective area of 0.16 cm^2 was controlled by a mask. This dye-adsorbed TiO_2 photoanode and a CE were assembled to fabricate the DSSC. A gap of 25 μm was fixed between the two electrodes by using a tiny Surlyn® frame (Solaronix) as a spacer. An electrolyte containing 1.0 M DMPII, 50 mM LiI, 30 mM I_2, 0.1 M GuSCN, and 0.5 M TBP in AN/valeronitrile was then slowly injected through a hole between the electrodes by a capillary effect. A Pt-based CE (Pt-CE) was prepared by sputter-depositing Pt onto an FTO substrate, by using a Cressington 108 auto Sputter Coater (Cressington Scientific Instruments Ltd., Watford, UK); the sputtering was performed at 40 mA for 130 s.

2.4. Instrumentation

Thermo-gravimetric analyzer (TGA, TGA-7, Perkin–Elmer) was used for verifying the attachment of ANI monomers to GNs; for this a Philip Tecnai G^2 LaB6 Gun Transmission Electron Microscope with a Gatan Dual Vision CCD Camera was used, operating it at 200 keV. An UV/VIS/NIR spectrophotometer (V-570, Jasco) was used to analyze the effect of reflux condensation on the interactions between GN and ANI in the GN/ANI particle, and to analyze the dispersing behavior of particles of ANI/GN in an aqueous solution. FTIR spectra were obtained by a spectrum 100 PerkinElmer FTIR spectrometer (PerkinElmer, Inc.). The particle size of GN/ANI in the aqueous solution was observed by zeta-potential (Brookhaven Instruments Corporation). Surface morphologies of the CEs were observed by scanning electron microscopy (SEM, Nova™ NanoSEM 230). Raman spectra were recorded by a Dimension-P2 Raman System (Lamba Solution, Inc.). A CHI model 900B SECM (CH Instruments, Austin, TX) was employed to measure the electrochemical properties of the composite films. The DSSCs were illuminated by a class A quality solar simulator (PEC-L11, AM 1.5G, Peccell Technologies, Inc.), and the incident light intensity (100 mW cm^{-2}) was calibrated with a standard silicon cell (PECSI01, Peccell Technologies, Inc.). Photoelectrochemical characteristics of the DSSCs and their electrochemical impedance spectroscopic (EIS) spectra were

recorded with a potentiostat/galvanostat (PGSTAT 30, Autolab, Eco-Chemie, the Netherlands).

3. Results and discussion

3.1. Preparation of aniline (ANI) modified graphene (GN)

A solution containing ANI monomers and GNs was prepared first. The mixture was subjected to refluxing at 210 °C for 3 h. The refluxed solution was then filtered through an MF-Millipore mixed cellulose ester membrane to obtain a composite of GN/ANI. The TGA traces in Fig. 1 show that the mass of the GN/ANI particles starts to decrease significantly at about 150 °C, while the mass of pristine GN remains stable up to 500 °C. The loss in the weight of GN/ANI can be ascribed to the ANI monomers. This phenomenon confirms the presence of ANI in the GN/ANI particles. In addition, the obtained GN/ANI particles were observed by HR-TEM; the HR-TEM image in Fig. 1 shows that the GN/ANI particles are flat and transparent. The selected area electron diffraction (SAED) pattern inserted in the image of HR-TEM of the GN/ANI particles shows that the GN/ANI particles are crystalline in nature and possess similar crystalline pattern as that of graphite.

3.2. Dispersibility of GN/ANI particles in an aqueous solution

The effect of the refluxing process on the dispersibility of GN/ANI particles in an aqueous solution was studied. For comparative purpose, other GN/ANI particles were synthesized without using a reflux process (denoted as non-refluxed GN/ANI particles). The non-refluxed GN/ANI particles were prepared merely by mixing the GNs with the ANI monomers, without heating and refluxing. Fig. 2 shows the FTIR spectra of pristine GN, refluxed GN/ANI particles, and non-refluxed GN/ANI particles. Owing to the presence of ANI in the GN/ANI particles, characteristic bands of ANI can be seen in the FTIR spectra. The bands centered at 693, 754, and 1499 cm^{-1} are due to the aromatic ring bend, aromatic out-of-plane C—H bending, and aromatic ring mode, respectively [27]. In contrast, the mentioned bands cannot be seen in the spectrum of pristine GN. Moreover, the intensities of these bands for the refluxed GN/ANI particles are smaller than those for the non-refluxed GN/ANI particles. This may be due to the restrictions of modes of vibrations in ANI by some interactive forces developed between GN and ANI [28]. In addition, the UV/Vis absorption spectrum of refluxed particles of GN/ANI is exhibited in the inset of Fig. 2. An absorption

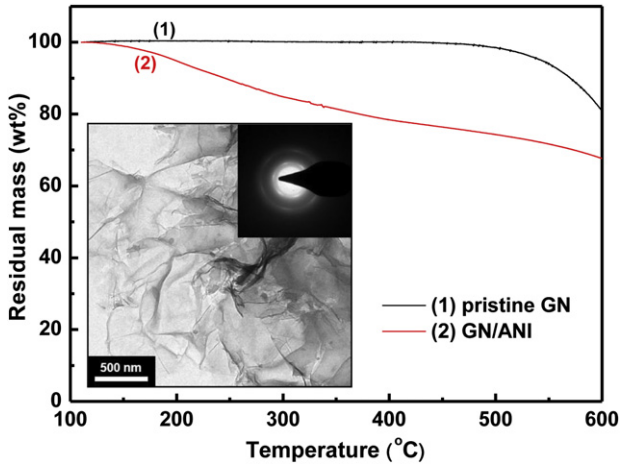

Fig. 1. TGA traces of pristine GN and GN/ANI particles. The inset shows the HR-TEM image of the particles of GN/ANI and their corresponding SAED pattern.

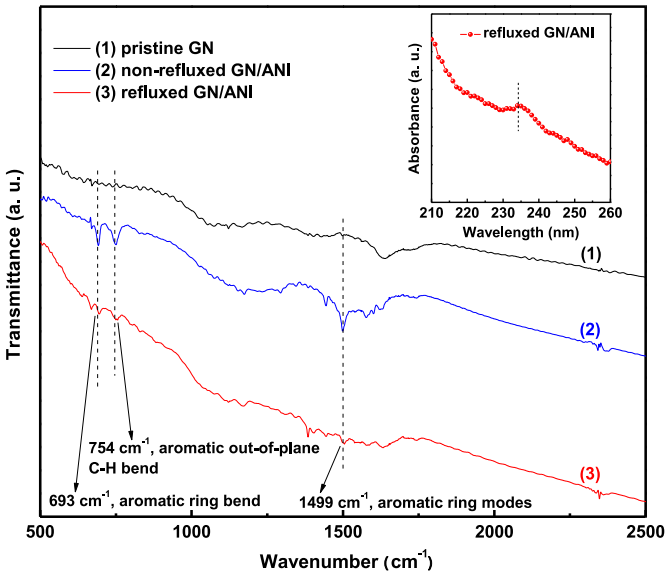

Fig. 2. FTIR spectra of pristine GN, refluxed GN/ANI particles, and non-refluxed GN/ANI particles. The inset shows UV/Vis absorption spectrum of GN/ANI particles.

peak centered at around 234 nm corresponds to the ANI of the refluxed GN/ANI particles. The results of UV/Vis absorption and FTIR indicate that there is an interactive force in the GN/ANI particles, prepared by using a reflux condensation.

The dispersibilities of refluxed and non-refluxed GN/ANI particles were studied by UV/Vis absorption spectroscopy; the spectra were obtained at 550 nm for a period of 9 h (Fig. 3a). The

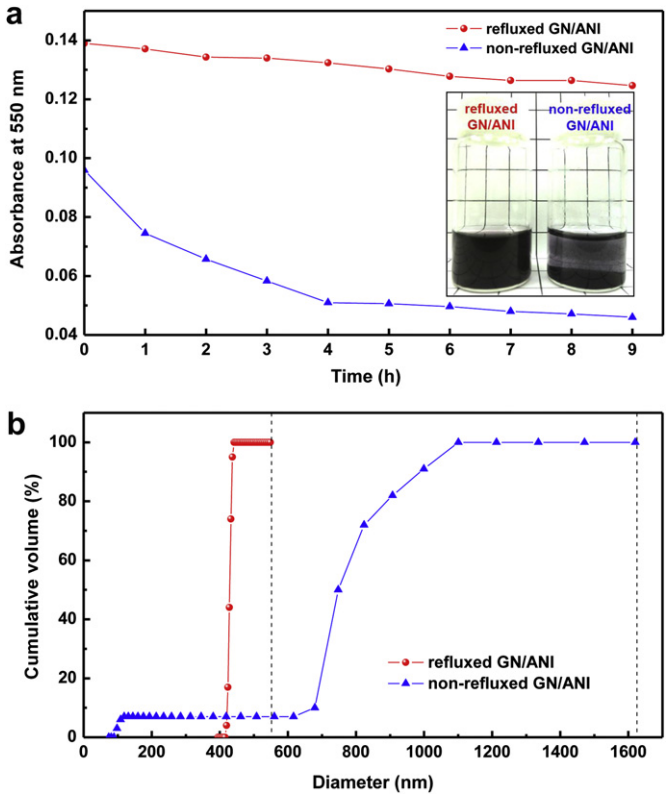

Fig. 3. (a) UV/Vis absorptions (@550 nm) of refluxed and non-refluxed GN/ANI particles, as functions of time; the inset of (a) shows their actual photographs. (b) Size distribution of refluxed and non-refluxed GN/ANI particles.

photographs of two vials consisting of refluxed and non-refluxed GN/ANI particles are shown in the inset of Fig. 3a. The absorbance (Abs) of 0.14 for the refluxed GN/ANI particles in an aqueous solution is higher than that of non-refluxed GN/ANI particles (Abs = 0.09) in their initial stages, indicating a good dispersion of the refluxed GN/ANI particles. The dispersing behavior of the refluxed GN/ANI particles in the aqueous solution is relatively steady for at least 9 h, while it is rickety for the same period in the case of non-refluxed GN/ANI particles (Fig. 3a). This may be attributed to the interactive force between GN and ANI. Under these conditions, the ANI can serve as a dispersant for the refluxed GN/ANI particles in an aqueous solution. There could have been an easy agglomeration of pristine GN, had there been only van der Waals force in the case of non-refluxed GN/ANI particles. Furthermore, the average size of refluxed GN/ANI particles in aqueous solution (diameter = 431.3 nm) was smaller and the particles were more uniform, compared with the size and uniformity of non-refluxed GN/ANI particles (diameter = 786.5 nm) (Fig. 3b). In Fig. 3b, the sharp slope of the curve of the refluxed GN/ANI particles indicates the uniformity of the particle size. These observations imply that there is an interactive force between GN and ANI in the case of refluxed GN/ANI particles.

3.3. Preparation and characterization of the composite film of GN/PANI

The composite thin film of GN/PANI was coated on an FTO substrate by electro-polymerization from a HCl solution containing the refluxed GN/ANI particles, which served as the monomers. The film of GN/PANI was then observed and examined by SEM and Raman spectra (Fig. 4). Fig. 4a shows plane view SEM image of pristine PANI film; the film has fiber-like aggregates of PANI. In Fig. 4b, the composite film of GN/PANI exhibiting that the fiber-shaped PANI is covered by GNs. On the other hand, a thin film of GN/PANI prepared from the non-refluxed GN/ANI particles through electro-polymerization exhibits the same surface morphology as that of pristine GN (SEM not shown), suggesting that no ANI monomers were attached to the GNs through this electro-polymerization. Fig. 4c shows Raman spectra of pristine GN, pristine PANI, and the composite film of GN/PANI. The characteristic peaks centered at around 1347 and 1578 cm^{-1} are ascribed to D and G bands, respectively, for the composite film of GN/PANI. Thus, the SEM images and the Raman spectra have confirmed the successful incorporation of GNs in the electro-polymerized composite film of GN/PANI.

3.4. Photovoltaic performances of the DSSCs with various CEs

CEs were prepared with GN/PANI by electro-polymerization, by adding specific percentage of GN to prepare the GN/ANI particles (0.02, 0.05, 0.10, and 0.20 wt%) and also by applying different charge capacities (20, 40, 60, and 80 mC cm^{-2}); Fig. 5 shows the power-conversion efficiencies (η) of the DSSCs fabricated using such CEs. Each value of η is an average of three measurements. Fig. 5a shows that the optimal weight percentage of GNs to be used for preparing the particles of GN/ANI (for using in the refluxing solution) is 0.05 wt%; Fig. 5b shows that the optimal charge capacity for depositing the film of GN/PANI for a CE is 40 mC cm^{-2}. At a low charge capacity (20 mC cm^{-2}), the FTO substrate is not expected to be fully covered with a layer of GN/PANI, which may decrease the fill factor (*FF*) of the corresponding DSSC. At higher charge capacities (60, and 80 mC cm^{-2}), the internal resistances of the films for electron transfer are expected to increase. At a charge capacity of 40 mC cm^{-2}, the DSSC with 0.05 wt% of GN shows the highest efficiency of 7.17% (Table 1); this implies that the corresponding composite film of GN/PANI has the largest active surface area at this concentration of GNs.

Photocurrent density–voltage (*J–V*) characteristics of the DSSCs with CEs with the films of GN/PANI (GN/PANI-CE, 40 mC cm^{-2}, 0.05 wt% GN), pristine PANI (PANI-CE), pristine GN (GN-CE), and sputtered Pt (Pt-CE) are shown in Fig. 6. Their corresponding photovoltaic parameters are summarized in Table 1. The short-

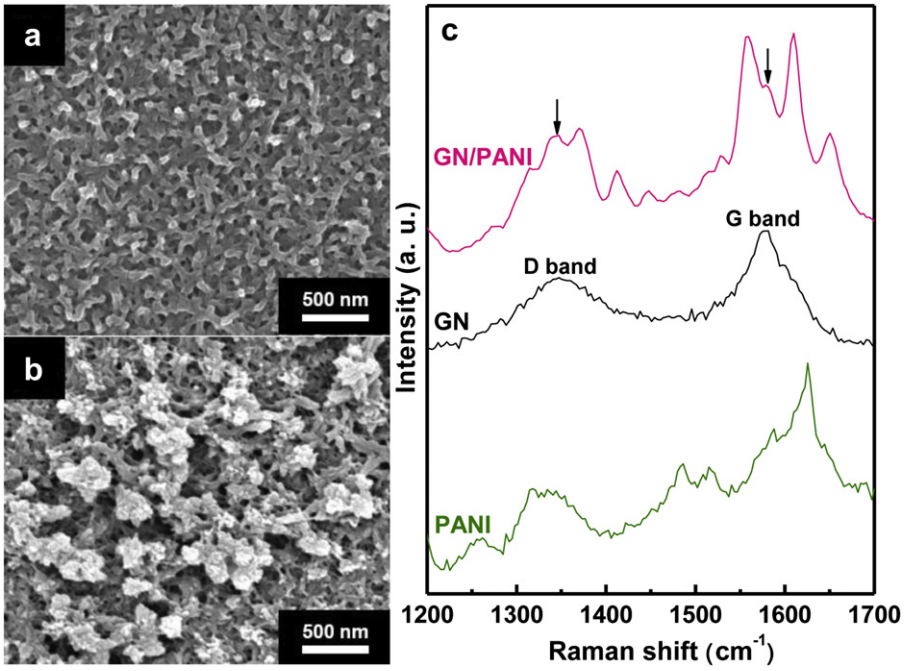

Fig. 4. Plane view SEM images of films of (a) pristine PANI and (b) GN/PANI, both prepared by electro-polymerization. (c) Raman spectra of films of GN/PANI, pristine GN, and pristine PANI.

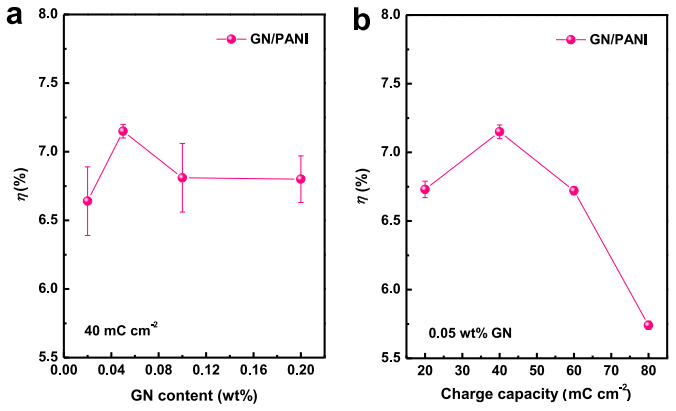

Fig. 5. Power-conversion efficiencies (η) of the DSSCs as the functions of (a) GN content for preparing the particles of GN/ANI (for using in the refluxing solution) and (b) charge capacity used for the electro-polymerization of the composite film of GN/PANI.

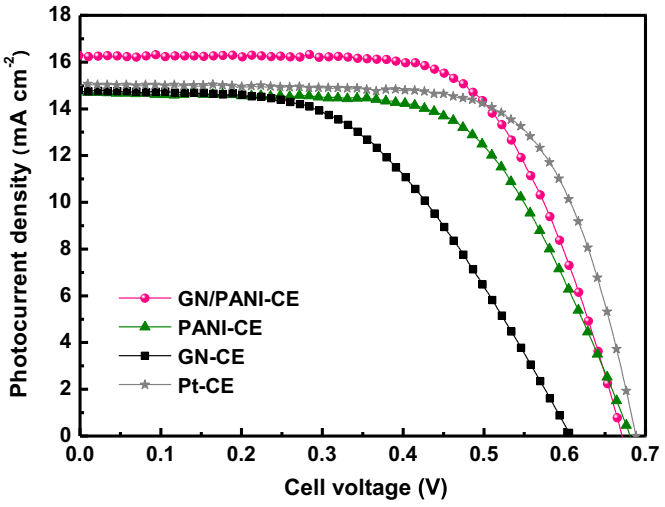

Fig. 6. Photocurrent density–voltage (J–V) characteristics of the DSSCs with CEs with the films of GN/PANI (40 mC cm^{-2}, 0.05 wt% GN), pristine PANI, pristine GN, and sputtered Pt, at 100 mW cm^{-2} illumination.

circuit current density (J_{SC}) (16.28 mA cm^{-2}), *FF* (0.67), and η (7.17%) of the DSSC with the catalytic film of GN/PANI are much higher than those of the DSSCs with the catalytic films of pristine PANI (J_{SC} = 14.68 mA cm^{-2}, *FF* = 0.63, and η = 6.27%) and pristine GN (J_{SC} = 14.79 mA cm^{-2}, *FF* = 0.50, and η = 4.54%). Compared with the case of the DSSC with the PANI-CE, such enhancements in favor of the cell with GN/PANI-CE are clearly due to the presence of GN in the composite film of GN/PANI, which can provide larger surface area for the composite film for the reduction of I_3^- ions; this observation is in accordance with the SEM images in Fig. 4 a and b; that is to say that a larger surface area leads to a higher electro-catalytic ability and thereby to a higher J_{SC} and higher η. On the other hand, the enhanced performance of the DSSC with GN/PANI-CE, compared with that of the DSSC with pristine GN-CE, is due to higher electro-catalytic ability of the CE with GN/PANI than that of the CE with pristine GN for the reduction of I_3^- ions; this higher electro-catalytic ability is demonstrated through CV analysis in further discussion. It is well-known that higher electro-catalytic ability of a CE leads to higher J_{SC}, which in this case has led to enhanced performance of the cell with GN/PANI-CE. Although the J_{SC} of the DSSC with GN/PANI-CE (16.28 mA cm^{-2}) is much higher than that of the cell with bare Pt-CE (15.01 mA cm^{-2}), the η of the DSSC with GN/PANI-CE (7.17%) is just close to the η of cell using Pt-CE (7.24%); this is obviously to be attributed to the higher values of *FF* and open-circuit voltage (V_{OC}) in favor of the cell with Pt. Pt being a metal is expected to have higher electronic conductivity than that of GN/PANI; this higher electronic conductivity leads to a lower charge transfer resistance at its surface and thereby to a higher *FF* for the cell with Pt-CE. It can be seen in further discussions through CV that the CE with Pt has a higher electro-catalytic ability than that of the CE with GN/PANI; this higher electro-catalytic ability of the CE with Pt implies faster reduction of I_3^- ions at its surface, which means a reduction of recombination between conduction band electrons and I_3^- ions, and thereby a higher V_{OC} in favor of the cell with Pt-CE. The relatively porous morphology of GN/PANI film (see Fig. 4b), with reference to the dense surface morphology of Pt, can hinder the charge transfer at the film of GN/PANI, and this charge transfer resistance may be a reason for the smaller *FF* (0.67) in the case of the cell with GN/PANI-CE, compared to that of the cell with Pt-CE. (0.70); it is demonstrated through EIS in further discussion that the interfacial charge-transfer resistance (R_{ct}) is 0.64 Ω cm^2 in the case of GN/PANI film, while it is 0.22 Ω cm^2 in the case of Pt film (Table 1).

Table 1
Photovoltaic parameters of the DSSCs with CEs with the films of GN/PANI (40 mC cm^{-2}, 0.05 wt% GN), pristine PANI, pristine GN, and sputtered Pt, at 100 mW cm^{-2} illumination. These performance parameters are also related to the peak separation (E_p) and interfacial charge-transfer resistance (R_{ct}) of these films.

Catalytic CE films	V_{OC} (V)	J_{SC} (mA cm^{-2})	*FF*	η (%)	E_p (mV)	R_{ct} (Ω cm^2)
GN/PANI	0.67	16.28	0.67	7.17	206	0.64
PANI	0.68	14.68	0.63	6.27	270	0.72
GN	0.60	14.79	0.50	4.54	325	1.46
Pt	0.69	15.01	0.70	7.24	186	0.22

3.5. Electro-catalytic abilities of various CEs by CV and EIS

An Ag/Ag$^+$ electrode and a Pt foil were used as the reference and the counter electrode, respectively, for subsequent CV analyses. CV curves were obtained in an AN-based electrolyte, containing 0.01 M LiI, 1.0 mM I_2, and 0.1 M $LiClO_4$, at a scan rate of 50 mV s^{-1} to estimate the electro-catalytic abilities of CEs with various films. In Fig. 7a, each CV curve shows an anodic peak current density (I_{pa}) and a cathodic peak current density (I_{pc}), corresponding to the oxidation of I^- ions and the reduction of I_3^- ions, respectively. The electrochemical reaction at the interface of a catalytic film and its electrolyte in a DSSC is represented as follows:

$$I_3^- + 2e^- \rightarrow 3I^- \quad (1)$$

Based on the magnitude of I_{pc}, the electro-catalytic ability of the CE with GN/PANI is lesser than that of the CE with sputtered Pt (Fig. 7a). In addition, the higher electro-catalytic ability of the CE with Pt is found to be in consistency with its lower peak separation (E_p) of 186 mV, with reference to that of the CE with GN/PANI (E_p = 206 mV, Fig. 7a and Table 1). This decreased value of E_p indicates that the charge transfer kinetics of the redox reaction of I^-/I_3^- ions at the CE with Pt are faster than those at the CE with GN/PANI.

The electro-catalytic properties of these films were also studied by EIS, as shown in Fig. 7b. EIS spectra were obtained for CEs with different catalytic films, using in each case a symmetric cell containing two identical counter electrodes. The geometrical surface area of each film was fixed to be 1.0 cm^2. The distance between the electrodes of the symmetric cell was fixed to be 25 μm by using a tiny Surlyn® frame. For the preparation of the film of GN/PANI or PANI, in the case of a symmetric cell, the pattern was controlled to

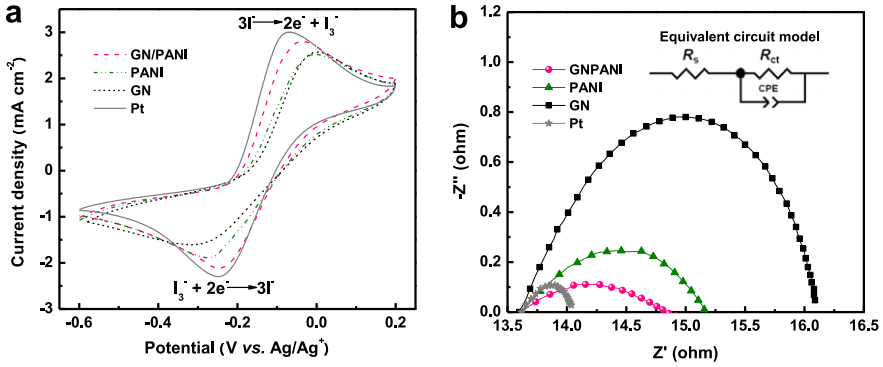

Fig. 7. (a) CV curves of CEs with GN/PANI, pristine PANI, pristine GN, and sputtered Pt; (b) EIS spectra of these CEs.

have the size of 1.0 cm^2 on the surface of the FTO glass, using a non-conducting Surlyn®. That is, the residual area of the FTO glass was covered with Surlyn®. Thus, the formation of these films through electro-polymerizing occurred only on the conducting surface area of 1.0 cm^2 of the FTO glass. In addition, the electrolyte used was the same as that in a DSSC. A frequency range of 40 kHz–100 Hz was used to estimate the interfacial charge-transfer resistance (R_{ct}) in a cell. The value of R_{ct} for a symmetric cell is half of the value of diameter (on the *X*-axis) of its corresponding semicircle (Fig. 7b). The values of R_{ct} for various films are summarized in Table 1. The lowest value of $R_{ct} = 0.22\ \Omega\ cm^2$ in the case of sputtered Pt (Table 1) is in accordance with its highest electro-catalytic ability (see Fig. 7a). The R_{ct} values follow the trend: sputtered Pt (0.22 Ω cm^2) < GN/PANI composite film (0.64 Ω cm^2) < pristine PANI (0.72 Ω cm^2) < pristine GN (1.46 Ω cm^2); this trend is in consistency with the corresponding electro-catalytic abilities and peak separations (see Fig. 7a and Table 1). It is thus confirmed that the composite film of GN/PANI has a higher electro-catalytic ability than those of pristine PANI film and pristine GN film. The η of the DSSCs are in consistency with the electro-catalytic abilities of their CEs (see the cathodic peaks in Fig. 7a) and also with the charge transfer resistance and peak separation of the CEs (see Table 1).

The above results suggest that the composite film of GN/PANI is a potential alternative to the conventional, expensive Pt film for a DSSC.

4. Conclusions

A composite of GN/ANI was obtained from a solution of ANI monomer and GN by refluxing the solution. According to UV/Vis absorption spectra, the dispersions and stabilities of refluxed GN/ANI particles are higher than those of non-refluxed GN/ANI particles in aqueous solution. FTIR spectra show a stronger interaction between ANI and GN in the case of refluxed particles of GN/ANI, than that in the case of non-refluxed particles of GN/ANI. Composite thin films of GN/PANI were successfully deposited on FTO substrates by electro-polymerization. Raman spectra and SEM images have confirmed the formation of the composite film of GN/PANI on the FTO substrate from the refluxed GN/ANI particles. The composite thin film of GN/PANI derived from the GN/ANI particles exhibited higher surface area, with reference to that of the film of pristine PANI. The optimal percentage of GN to be used for preparing the particles of GN/ANI (for using in the refluxing solution) is 0.05 wt%, and the optimal charge capacity for depositing the film of GN/ANI for a CE is 40 mC cm^{-2}. Higher J_{SC} and lower *FF* were obtained for the DSSC with GN/PANI-CE, as compared with those of the DSSC with Pt-CE. The DSSC with GN/PANI-CE (40 mC cm^{-2}) shows an η of 7.17%, which is comparable to that of a DSSC with Pt-CE (η = 7.24%). The composite film of GN/PANI has a higher electro-catalytic ability than those of pristine PANI film and pristine GN film, however a lower electro-catalytic ability than that of sputtered Pt film. The above results suggest that the composite film of GN/PANI is a potential alternative to the conventional, expensive Pt film for a DSSC.

Acknowledgments

This work was financially supported by the National Science Council and the Academia Sinica of Taiwan.

References

[1] B. O'Regan, M. Grätzel, Nature 353 (1991) 737–740.
[2] X. Mei, S.J. Cho, B. Fan, J. Ouyang, Nanotechnology 21 (2010) 395202.
[3] G. Veerappan, K. Bojan, S.W. Rhee, ACS Appl. Mater. Interfaces 3 (2011) 857–862.
[4] J. Chen, K. Li, Y. Luo, X. Guo, D. Li, M. Deng, S. Huang, Q. Meng, Carbon 47 (2009) 2704–2708.
[5] L. Wan, S. Wang, X. Wang, B. Dong, Z. Xu, X. Zhang, B. Yang, S. Peng, J. Wang, C. Xu, Solid State Sci. 13 (2011) 468–475.
[6] H. Choi, H. Kim, S. Hwang, W. Choi, M. Jeon, Sol. Energy Mater. Sol. Cells 95 (2011) 323–325.
[7] J.D.R. Mayhew, D.J. Bozym, C. Punckt, I.A. Aksay, ACS Nano 4 (2010) 6203–6211.
[8] K.S. Novoselov, A.K. Geim, S.V. Morozov, D. Jiang, Y. Zhang, S.V. Dubonos, I.V. Grigorieva, A.A. Firsov, Science 306 (2004) 666–669.
[9] A.K. Geim, K.S. Novoselov, Nat. Mater. 6 (2007) 183–191.
[10] A.K. Geim, P. Kim, Sci. Am. 298 (2008) 90–97.
[11] J.G. Chen, H.Y. Wei, K.C. Ho, Sol. Energy Mater. Sol. Cells 91 (2007) 1472–1477.
[12] A. Kanciurzewska, E. Dobruchowska, A. Baranzahi, E. Carlegrim, M. Fahlman, M.A. Gîrţu, J. Optoelectron. Adv. Mater. 9 (2007) 1052–1059.
[13] K.M. Lee, C.Y. Hsu, P.Y. Chen, M. Ikegami, T. Miyasaka, K.C. Ho, Phys. Chem. Chem. Phys. 11 (2009) 3375.
[14] J. Wu, Q. Li, L. Fan, Z. Lan, P. Li, J. Lin, S. Hao, J. Power Sources 181 (2008) 172–176.
[15] S.S. Jeon, C. Kim, J. Ko, S.S. Im, J. Mater. Chem. 21 (2011) 8146–8151.
[16] J. Zhang, T. Hreid, X. Li, W. Guo, L. Wang, X. Shi, H. Su, Z. Yuan, Electrochim. Acta 55 (2010) 3664–3668.
[17] Q. Qin, J. Tao, Y. Yang, Synth. Met. 160 (2010) 1167–1172.
[18] A.G. MacDiarmid, Curr. Appl. Phys. 40 (2001) 2581–2590.
[19] T. Kang, K.G. Neoh, K.L. Tan, Prog. Polym. Sci. 23 (1998) 277–324.
[20] W. Hong, Y. Xu, G. Lu, C. Li, G. Shis, Electrochem. Commun. 10 (2008) 1555–1558.
[21] H. Sun, Y. Luo, Y. Zhang, D. Li, Z. Yu, K. Li, Q. Meng, J. Phys. Chem. C 114 (2010) 11673–11679.
[22] J. Zhang, X. Li, W. Guo, T. Hreid, J. Hou, H. Su, Z. Yuan, Electrochim. Acta 56 (2011) 3147–3152.
[23] K. Kitamura, S. Shiratori, Nanotechnology 22 (2011) 195703.
[24] G. Wang, J. Yang, J. Park, X. Gou, B. Wang, H. Liu, J. Yao, J. Phys. Chem. C 112 (2008) 8192–8195.
[25] A. Dideykin, A.E. Aleksenskiy, D. Kirilenko, P. Brunkov, V. Goncharov, M. Baidakova, D. Sakseev, A.Y. Vul, Diam. Relat. Mater. 20 (2011) 105–108.
[26] C.Y. Chen, M. Wang, J.Y. Li, N. Pootrakulchote, L. Alibabaei, C. Ngoc-le, J.D. Decoppet, J.H. Tsai, C. Grätzel, C.G. Wu, S.M. Zakeeruddin, M. Grätzel, ACS Nano 3 (2009) 3103–3109.
[27] B.C. Smith, Infrared Spectral Interpretation: A Systematic Approach, CRC Press, New York, 1998.
[28] I. Kanesaka, T. Miyajima, K. Kawai, J. Mol. Struct. 118 (1984) 189–195.